A MONOLITHIC 35 GHz HBT QUASI-OPTICAL GRID OSCILLATOR

E.A. Sovero[a], Moonil Kim[b], R.M. Weikle II*[b], D.S. Deakin[a], W.J. Ho[a], J.A. Higgins[a], D.B. Rutledge[b]

a Rockwell International, Science Center, 1049 Camino dos Rios, Thousand Oaks CA 91360
b Division of Engineering and Applied Science, California Institute of Technology, Pasadena CA 91125
* Present address: Dept. of Applied Electron Physics, Chalmers University of Technology, S 412 96 Goteborg, SWEDEN

INTRODUCTION

We report the fabrication and testing of a monolithic 35 GHz grid oscillator. The frequency of operation was 34.6 GHz at 13 dbm estimated ERP (equivalent radiated power). The device consists of an array of 6 by 6 HBT unit cells. The chip dimension was 6 mm by 7 mm. This is the first reported monolithic Grid oscillator at any frequency. Oscillators of this kind utilize the free-space propagation characteristics of electromagnetic beams to synchronize the operation of many spatially separated devices. Grid devices use optical techniques to provide electrical functions such as feedback and power combining. The frequency of operation is determined by the dimension of the unit cell and by the distance from the reflecting (feedback) back mirror. Higher frequencies require smaller unit cells, thus opening the possibility of very compact high power millimeter-wave sources.

Quasi-optical grid devices including oscillators, multipliers, mixers, and beam steerers have been demonstrated [1,2,3,4]. Motivation for studying quasi-optical devices is twofold: free-space power combining is more efficient at high frequencies than power combining in guided wave structures; and transmitting and receiving systems based on monolithic implementations of quasi-optical elements have the potential to be smaller, lighter, and substantially less costly than conventional phased-array systems. Grid oscillators interact with electric fields propagating in the direction normal to the grid substrate. By interacting in parallel, they overcome the inefficiencies of standard microstrip power combining. The grid structure serves the dual function of bias interconnect as well as the radiating element.

SELF-ALIGNED HBT FABRICATION

The typical layer structure of an AlGaAs/GaAs HBT for microwave power application is shown in Table 1. Carbon was used as the base layer p-type dopant for its low atomic diffusivity, higher doping concentration capability, and higher hole mobility. Silicon was used as n-type dopant. Collector thickness and doping were designed to operate the device at above 8 volts. The base doping was chosen to be greater than $3 \times 10^{19} cm^{-3}$ to achieve high frequency performance and the base thickness was chosen to have high current bandwidth f_T. Emitter layer structure was optimized to balance the junction breakdown and the current gain. The emitter GaAs cap was heavily doped to $> 4 \times 10^{18} cm^{-3}$. Alternatively, a non alloyed InGaAs layer contact was used to achieve lower emitter contact resistance and to enhance the ohmic contact stability.

Table 1
Typical Epitaxial Structure of MOCVD Grown AlGaAs/GaAs HBT with Carbon-doped Base

Composition	Thickness (Å)	Doping (cm^{-3})	Function
n+ GaAs	1500 - 2500	$4 - 5 \times 10^{18}$	Cap
n- $Al_{.25}Ga_{.75}As$	700 - 1200	$3 - 7 \times 10^{17}$	Emitter
p+ GaAs	500 - 1000	$3 - 6 \times 10^{19}$	Base
n- GaAs	5000 - 9000	$3 - 8 \times 10^{16}$	Collector
n+ GaAs	6000 - 9000	$4 - 5 \times 10^{18}$	Sub-collector

After epitaxial growth, the AlGaAs/GaAs HBTs were fabricated with a self-aligned dual lift-off process [5,6,7]. The n-type contacts to the emitter and collector layers and p-type contact to the base layer were formed by evaporating AuGe/Ni/Au and Ti/Pt/Au, respectively. The standard Rockwell MIMIC process was used. This process, geared for microstrip circuits, includes two levels of metal interconnect , air bridge crossovers, MIM capacitors, thin film NiCr resistors and through-substrate-vias. These last three items were not required in the fabrication of the grid oscillator but nevertheless are available. Finally the wafer was thinned down to 4 mils.

The self-aligned process, shown in cross section in Fig. 1, enhances the device performance through the reduction of the base resistance and the base-collector capacitance. The base-collector capacitance was further reduced by implanting the collector in the extrinsic base region with protons. The base resistance and the base-collector capacitance for a typical device with emitter area of 40 μm^2 were estimated to be 10 Ω and 35 fF respectively, which were lower than those from a representative non self-aligned device of similar emitter dimensions by 30% [5,6].

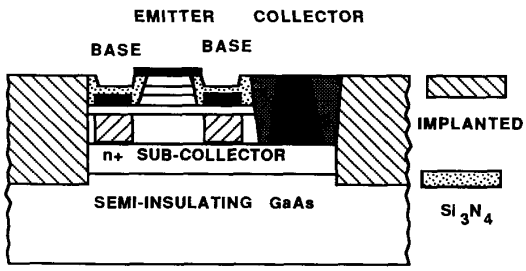

Fig. 1. Device cross section of a self- aligned HBT.

0-7803-0773-9/92 $3.00 © 1992 IEEE

The dc characteristics and rf performance were measured on the devices with two 1.8 μm by 9 μm emitter fingers. The offset voltage is less than 0.2V and knee voltage is around 0.5V at current density of 1 KA/cm^2. HBTs always achieve hard breakdown; BV_{cbo} is 20V and BV_{ceo} is above 12V for the devices with 0.7 μm collector thickness, and is usually within 1V across a 3-inch wafer. The distribution of Gummel plots across a 3-inch wafer shows uniform base-emitter turn-on voltage Vbe of 1.278+/-4 mV at a current density of 300A/cm^2 and uniform hfe of 31.0 +/-2.2 at of 50 KA/cm^2.

The devices reported here are implant isolated and have an emitter active area of 40 square microns each. The transistors when measured with a wafer RF probe exhibit f_T = 65 GHz and f_{max} = 90 GHz.

GRID OSCILLATOR DESIGN

The grid unit cell was 1 mm by 1 mm. The transistor is placed in the center of the cell at the intersection of 40 μm wide lines. The two vertical leads connect the emitter on one side and the collector on the other (Fig. 2). The two horizontal lines connect to the base. In this common base configuration both the "input" emitter and "output" collector leads are oriented vertically with the reflecting mirror completing the feedback loop.The resulting electric field polarization is also in this vertical direction. This pattern repeats six times vertically and horizontally, alternating the orientation of the devices to connect the emitters and collectors of adjacent rows in a common bus to make up the full grid. Figure 3 shows a photograph of the completed grid. Electrically the transistors are all connected in parallel (in common base configuration) as shown in Fig. 4. The 0.004" thick grid chip was mounted on a 0.025" GaAs substrate. This second substrate was metallized on the back to create the reflecting (feedback element) mirror. No additional tuning elements are present. The total stack height 0.029" (Fig. 5) was then mounted on a 64 pin IC flat pack carrier shown in Fig. 6. Bias was applied to the chip with bond wires to the ends of each row. Bias lines were bypassed outside the chip carrier to eliminate the possibility of low frequency oscillations (typically X-band).

EXPERIMENTAL RESULTS

At the bias conditions 1.8 Vcb and -1.5Veb at 80ma, oscillations were observed at 34.6 GHz (Fig. 7). The effective radiated power (ERP) is 120 mW. The E-plane and H-plane patterns are shown in Fig. 8. The E-plane pattern is badly split. There are three lobes of almost equal strength. We attribute the source of this splitting to metal surfaces on the chip carrier holder that are proximate to the grid. On the other hand, the H-plane pattern is good. For comparison, the theoretical pattern for a uniformly illuminated aperture of the same width as the grid is shown on the H-plane plot. For the main beam, theory and experiment agree well, and the sidelobe levels are similar. The frequency of oscillation could be moved about hundred MHz with changes in bias. Additional frequency tuning as well as higher output power are possible by using a movable back reflector. In our current configuration the distance from the grid to the back reflector is fixed at 29 mils. The polarization of the signal was better than 20 db, indicating that oscillations were occurring in the predicted mode. A simple electro magnetic model [8] of the grid predicted oscillations at around 39 GHz. The model based on EMF theory calculates the equivalent impedance of the grid elements and its interaction with space. These impedances in conjunction with the HBT S-parameters

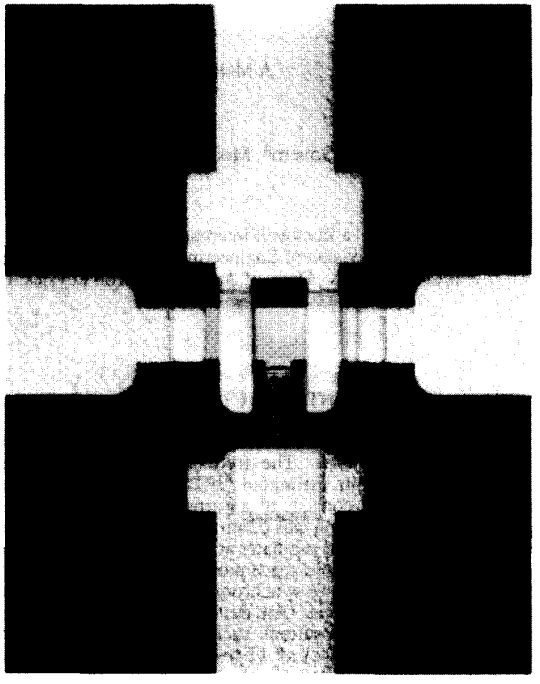

Fig. 2. Close-up of HBT at the center of a Grid Oscillator unit cell. The device has 2 emitter fingers 10 μm by 2 μm. The emitter and collector are connected to top and bottom leads while the base is connected to the two horizontal ones.

are then used to establish the frequency of oscillations. Figure 9 shows a PUFF simulation of the HBT grid oscillator. The difference of the predicted and measured frequency can be attributed to the assumptions used in the model (i.e., infinite array of elements).

CONCLUSIONS

The initial results presented here open up a new area in power generation at millimeter wave frequencies. Small but high gain devices can be combined easily and efficiently to generate large amounts of power, of the order of watts. At higher frequencies, the unit cell size decreases and thus the power density increases. Grid oscillators require a very simple bias arrangement, thus compact inexpensive millimeter wave sources could be built with standard monolithic techniques. The cell size is proportional to RF wavelength, so that the total cell density is proportional to the frequency squared. Possibilities of beam steering are also available and will be explored in the near future.

REFERENCES

[1] Z.B. Popovic, M. Kim, D.B. Rutledge, "Grid Oscillators," *Int. J. Infrared and Millimeter Waves* , Vol. 9, No. 7, pp 647-654, 1988.

[2] R.J. Hwu, L.P. Sadwick, N.C. Luhmann, D.B. Rutledge, M. Sokolich, B. Hancock, "Theoretical and Experimental Investigation of Watt-Level Wafer Scale Integration of Microwave and Millimeter-Wave GaAs and AlGaAs Frequency Multipliers," *47th Device Research Conference*, Boston, MA, June 1989.

[3] J.B. Hacker, R.M. Weikle II, M. Kim, M.P. DeLisio, D.B.Rutledge, "A 100-Element Planar Schottky Diode Grid Mixer," *IEEE Trans. Microwave Theory and Tech.*, Vol 40, No. 3, March 1992.

[4] M. Kim, R.M. Weikle II, J.B. Hacker, D.B. Rutledge, "Beam Diffraction by a Planar Grid Structure at 93 GHz," *IEEE Antenna and Propagation Society Symposium*, London, Ontario, June 1991.

[5] F. Chang, et al "AlGaAs/GaAs Heterojunction Bipolar Transistors Fabricated Using a Self-Aligned Dual-Lift-Off Process," IEEE EDL, Vol. EDL-8, No. 7, July 1987.

[6] W.J. Ho, M.F. Chang, N.H. Sheng, N.L. Wang, P.M. Asbeck, K.C. Wang, R.B. Nubling, G.J. Sullivan, and J.A. Higgins, "A Multifunctional HBT Technology," IEEE GaAs IC Symp. Technical Digest, pp 67-70, 1990.

[7] W.J. Ho, N.L. Wang, M.F. Chang, A. Sailer, and J.A. Higgins, "Self-Aligned, Emitter-Edge-Passivated AlGaAs/GaAs Heterojunction Bipolar Transistors with Extrapolated Maximum Oscillation Frequency of 350 GHz," 50th Annual DRC Technical Digest, IVA-1, 1992.

[8] R.M.Weikle II "Quasi-Optical Planar Grids for Microwave and Millimeter Wave Power Combining," PhD thesis, California Institute of Technology, Pasadena, CA, Nov-20th 1991.

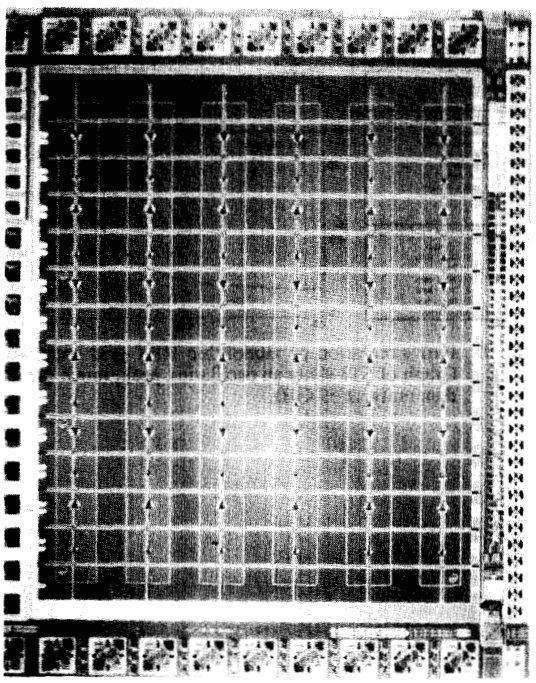

Fig. 3. Completed grid oscillator circuit. Grid dimensions are 7mm by 6mm (1 mm by 1mm unit cell).

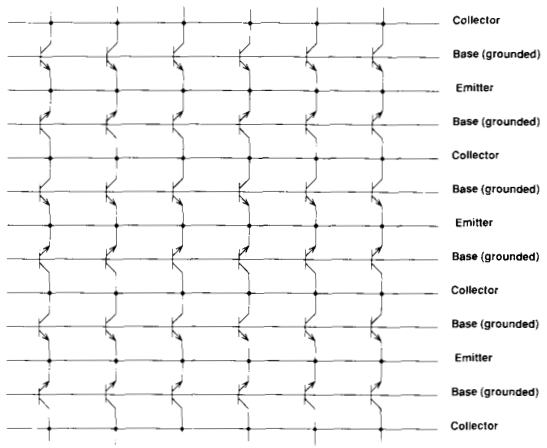

Fig. 4. Electrical equivalent circuit of grid. Note that electrically all devices are connected in parallel.

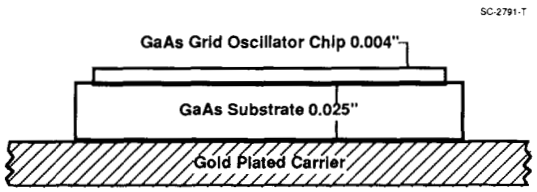

Fig. 5. Cross section of Ka-band grid oscillator assembly.

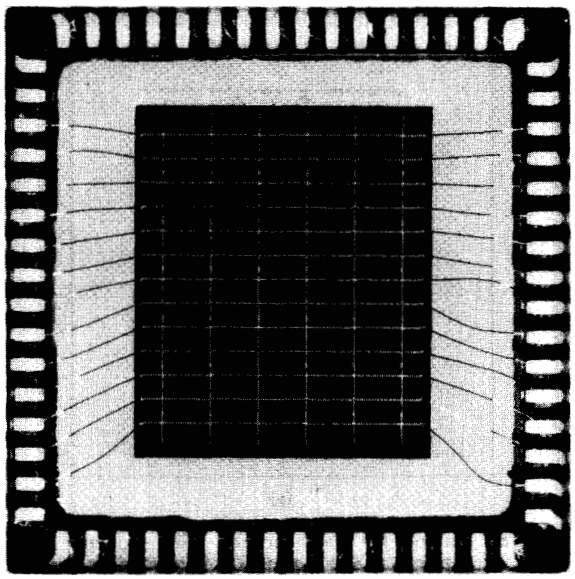

Fig. 6. Grid oscillator mounted in chip carrier.

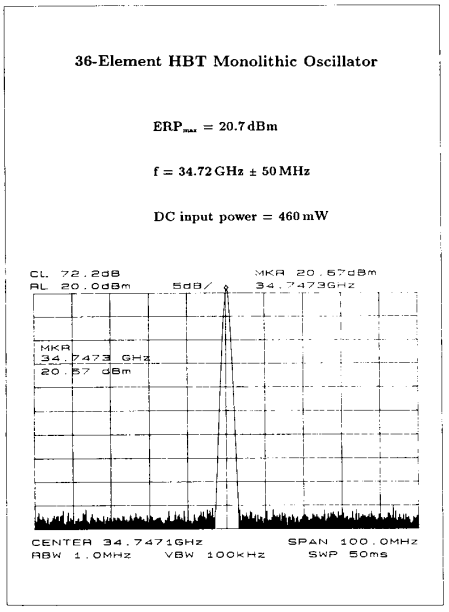

Fig. 7. Frequency spectrum of Grid Oscillator. No other frequency peaks were observed between 100 MHz and 50 GHz.

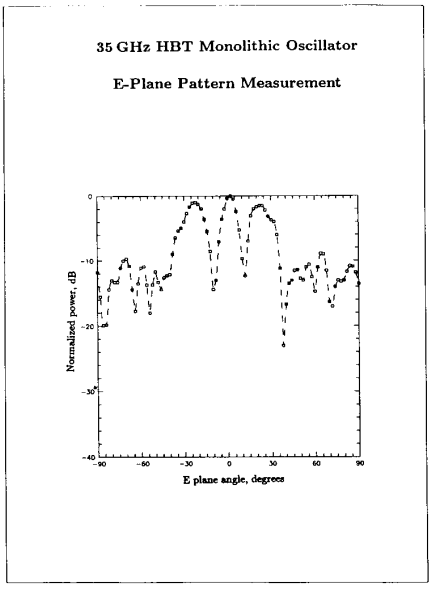

(a)

Fig. 8. Patterns for the monolithic HBT oscillator grid. E-plane (a) and H-plane (b). The solid line on the H-plane pattern is the pattern of a uniformly illuminated aperture with the same width as the grid.

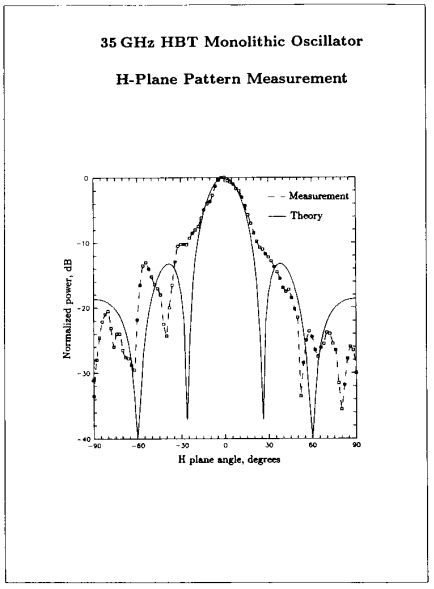

(b)

Fig. 8 (Continued)

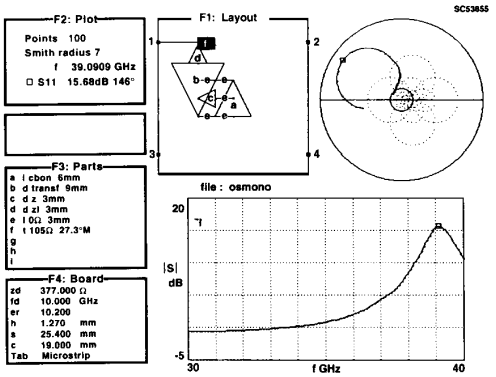

Fig. 9. Puff simulation of monolithic HBT grid oscillator. Graph of S11 show an oscillating peak, much greater than unity, at 39 GHz.